Trends in Computational and Applied Mathematics, **25** (2024), e01805
Sociedade Brasileira de Matemática Aplicada e Computacional
Online version ISSN 2676-0029 www.scielo.br/tcam
ORIGINAL ARTICLE
doi: 10.5540/tcam.2024.025.e01805

Parameter Identification Problem in the discrete-time SIR Model

JEMY A. MANDUJANO VALLE[1] and ALEXANDRE L. MADUREIRA[2]

Received on January 29, 2024 / Accepted on August 13, 2024

ABSTRACT. We investigate the problem of determining time dependent parameters for discrete-time epidemiological compartmental models such as the Susceptible-Infected-Recovered (SIR). We show how to determine parameters based on minimal error type iterative schemes. Such methods involve the computation of the adjoint of the derivative operator of a nonlinear function. This is a nontrivial task that we accomplish by carefully crafting auxiliary problems. To show the efficiency of the method, we consider examples involving real COVID-19 data.

Keywords: COVID-19, discrete SIR model, parameter estimation, inverse problem, minimal error method.

1 INTRODUCTION

Compartmental models for infectious diseases are pervasive in theoretical epidemiology, and became even more popular when the scientific community was faced with the challenge of predicting the dynamics of the COVID-19 pandemics. However, concealed in the models apparent simplicity, there is the difficult problem of determining time dependent parameters. In the case of diseases that affect humans, this is even more subtle since people's behavior depend on the very dynamics of the disease, government policies, etc. Given enough data, computational methods provide tools to determine parameters, even when the data is noisy.

The Susceptible-Infected-Recovered SIR model is one of the simplest and commonly used epidemiological models [20], and many authors use SIR-like models to analyze and estimate the dynamics of various diseases such as Ebola, HIV and Zika viruses [11, 19, 22] among many others. See [14] for details on compartmental models and a through review of the last century literature, and [10] for more recent literature, specially related to COVID-19 modeling.

In our variant of SIR model, the susceptibles are part of the total population that is healthy but at risk of becoming infected. The infected are those who have and might transmit the disease. Those

*Corresponding author: Jemy A. Mandujano Valle – E-mail: jhimyunac@gmail.com
[1]Laboratório Nacional de Computação Científica, Av. Getulio Vargas, 333, Quitandinha, Petrópolis, RJ, Brazil – E-mail: jhimyunac@gmail.com https://orcid.org/0000-0002-3732-6034
[2]Laboratório Nacional de Computação Científica, Av. Getulio Vargas, 333, Quitandinha, Petrópolis, RJ, Brazil/EPGE Escola Brasileira de Economia e Finanças – E-mail: alm@lncc.br https://orcid.org/0000-0002-8493-4905

who recover are immune, and, for simplicity, those who die are also counted as "recovered." We assume that the population is homogeneous, and that the initial number of infectious patients is known.

Since the outbreak of COVID-19, a considerable number of studies related to the computational modeling of the evolution of COVID-19 have been published, often based on SIR-like compartmental models. Regarding parameter estimation, [12, 15, 30] use the maximum likelihood method to estimate the basic reproduction method. The basic reproduction number is also estimated in [7, 24, 28], but this time based on the least square method. Different techniques to estimate several parameters from real data are considered in the literature, as statistical based arguments [2,3,4], machine learning [5,6], or genetic algorithms [1]. See also [9,26] for interesting considerations and other approaches.

In this work we propose a new method to estimate the basic time dependent reproduction number, among other parameters. The method can be extended to other compartmental models, e.g. SIRD, SEIR and SEAIR.

Consider a population of size $P > 0$. The discrete time SIR compartmental model determines for all discrete time $j = 1, 2, 3, \ldots$, the size of the susceptible population $\mathcal{S}_j$, the number of infectious $\mathcal{I}_j$, and the size of the "removed" population $\mathcal{R}_j$. Let $S_j = \mathcal{S}_j/P$ be the susceptible fraction of the population, $I_j = \mathcal{I}_j/P$ the infected fraction of the population, and $R_j = \mathcal{R}_j/P$ the recovered fraction of the population. The dynamics is determined by

$$\begin{aligned} S_{j+1} &= S_j - \beta_j I_j S_j, \\ I_{j+1} &= I_j + \beta_j I_j S_j - \gamma_j I_j, \\ R_{j+1} &= R_j + \gamma_j I_j. \end{aligned} \tag{1.1}$$

The initial conditions are determined by a given I_1 infected individuals (to avoid trivialities, we assume that I_1 is positive and smaller than 1), and $S_1 = 1 - I_1$, and $R_1 = 0$. Note that at all times, $S_j + I_j + R_j = 1$, reflecting the assumption that demographic changes are irrelevant due to the short time scale of the disease.

At a time j fixed, the parameters β_j and γ_j represent the probability of adequate contacts and the recovery probability [23]. We assume that both are unknown and we use the available data to estimate them. In our case, the data is the daily number of new infected individuals.

Note that these parameters are not available in practice, and it is hard (impossible?) to extract them directly from the data. But they are of paramount importance since they determine the dynamics of the disease. They also allow the computation of the basic and reproductive numbers, revealing whether the disease is subsiding or not. We present here a method to estimate those parameters, and show in two simulations, using real data, that the correct dynamics can be captured.

In what follows we summarize the contents of the article. In Section 2 we make some new definitions and describe how we handle the data. In Section 3, we define the Minimal Error Method, leaving the mathematical derivations for Section 4. Section 5 contains numerical tests

related to our method applied to two cities of different sizes, while Section 6 concludes the paper. Appendix A describes the smoothing method, and Appendix B outlines the Minimal Error Method in its generality.

2 HANDLING THE DATA

Consider that there are N days of data available, and let

$$\boldsymbol{B} = (\beta_1, \beta_2, \ldots, \beta_N)^T, \qquad \boldsymbol{\Gamma} = (\gamma_1, \gamma_2, \ldots, \gamma_N)^T, \qquad \boldsymbol{\Upsilon} = (1, 1, \ldots, 1)^T \in \mathbb{R}^N$$

$$\boldsymbol{o} = \begin{pmatrix} 0 \\ 0 \\ 0 \end{pmatrix}, \quad \boldsymbol{a}_j = \begin{pmatrix} S_j \\ I_j \\ R_j \end{pmatrix}, \qquad \boldsymbol{A} = \begin{pmatrix} \boldsymbol{a}_1 & \boldsymbol{o} & \ldots & \boldsymbol{o} \\ \boldsymbol{o} & \boldsymbol{a}_2 & \ldots & \boldsymbol{o} \\ \boldsymbol{o} & \boldsymbol{o} & \ldots & \boldsymbol{o} \\ \vdots & \vdots & \ddots & \vdots \\ \boldsymbol{o} & \boldsymbol{o} & \ldots & \boldsymbol{a}_N \end{pmatrix},$$

$$\boldsymbol{\Lambda} = \begin{pmatrix} \boldsymbol{a}_2 & \boldsymbol{o} & \ldots & \boldsymbol{o} \\ \boldsymbol{o} & \boldsymbol{a}_3 & \ldots & \boldsymbol{o} \\ \boldsymbol{o} & \boldsymbol{o} & \ldots & \boldsymbol{o} \\ \vdots & \vdots & \ddots & \vdots \\ \boldsymbol{o} & \boldsymbol{o} & \ldots & \boldsymbol{a}_{N+1} \end{pmatrix}, \quad \underline{0} = \begin{pmatrix} 0 & 0 & 0 \\ 0 & 0 & 0 \\ 0 & 0 & 0 \end{pmatrix}, \quad \boldsymbol{m}_j = \begin{pmatrix} 0 & -S_j & 0 \\ I_j & 0 & 0 \\ 0 & 0 & 0 \end{pmatrix},$$

$$\boldsymbol{M} = \begin{pmatrix} \boldsymbol{m}_1 & \underline{0} & \ldots & \underline{0} \\ \underline{0} & \boldsymbol{m}_2 & \ldots & \underline{0} \\ \underline{0} & \underline{0} & \ldots & \underline{0} \\ \vdots & \vdots & \ddots & \vdots \\ \underline{0} & \underline{0} & \ldots & \boldsymbol{m}_N \end{pmatrix}, \quad \boldsymbol{q} = \begin{pmatrix} 0 & 0 & 0 \\ 0 & -1 & 0 \\ 0 & 1 & 0 \end{pmatrix}, \qquad \boldsymbol{Q} = \begin{pmatrix} \boldsymbol{q} & \boldsymbol{o} & \ldots & \boldsymbol{o} \\ \boldsymbol{o} & \boldsymbol{q} & \ldots & \boldsymbol{o} \\ \boldsymbol{o} & \boldsymbol{o} & \ldots & \boldsymbol{o} \\ \vdots & \vdots & \ddots & \vdots \\ \boldsymbol{o} & \boldsymbol{o} & \ldots & \boldsymbol{q} \end{pmatrix}.$$

Then, (1.1) is equivalent to

$$\boldsymbol{\Lambda\Upsilon} = \boldsymbol{A\Upsilon} + \boldsymbol{MAB} + \boldsymbol{QA\Gamma}. \tag{2.1}$$

Assume that $\boldsymbol{I}^{cumul} = \left(I_1^{cumul}, I_2^{cumul}, \cdots, I_N^{cumul}\right)$ and $I_j{}^{cumul}$ is the cumulative number of infections on day j, resulting from smoothing the real data using exponential moving average techniques (EMA - details in the Appendix A). Let

$$\hat{S}_j = 1 - \frac{I_j^{cumul}}{P} \quad j = 1, 2, \ldots, N. \tag{2.2}$$

In this paper, we estimate $\boldsymbol{B}$ and $\boldsymbol{\Gamma}$ from (2.1), such that $S_1, \ldots, S_N$ is close to $\hat{S}_1, \ldots, \hat{S}_N$. In the following section, we describe how we do so.

3 MINIMAL ERROR METHOD

Let

$$\boldsymbol{d}_j = (S_j, 0, 0)^T \qquad \boldsymbol{D} = (\boldsymbol{d}_1, \boldsymbol{d}_2, \ldots, \boldsymbol{d}_N).$$

Consider the nonlinear operator $F:\mathbb{R}^{2N}\to\mathbb{R}^{3N}$ that takes the parameters $\boldsymbol{B}$ and $\boldsymbol{\Gamma}$ and returns $\boldsymbol{D}$, i.e., $\boldsymbol{D}=F(\boldsymbol{B},\boldsymbol{\Gamma})$, where (2.1) holds. Our goal is to find $(\boldsymbol{B},\boldsymbol{\Gamma})$ such that $\hat{\boldsymbol{D}}\approx\boldsymbol{D}=F(\boldsymbol{B},\boldsymbol{\Gamma})$. Here, $\hat{\boldsymbol{D}}$ is as $\boldsymbol{D}$ where S_j is replaced by $\hat{S}_j$.

We use an iterative method of Minimal Error Method type that, given $\hat{\boldsymbol{D}}$ and an initial guess $(\boldsymbol{B}^1,\boldsymbol{\Gamma}^1)$ determines a sequence $(\boldsymbol{B}^k,\boldsymbol{\Gamma}^k)$ by

$$(\boldsymbol{B}^{k+1},\boldsymbol{\Gamma}^{k+1})=(\boldsymbol{B}^k,\boldsymbol{\Gamma}^k)+\omega^k F'(\boldsymbol{B}^k,\boldsymbol{\Gamma}^k)^T(\hat{\boldsymbol{D}}-\boldsymbol{D}^k), \tag{3.1}$$

for $k=1,2,\ldots$, where $\boldsymbol{D}^k=F(\boldsymbol{B}^k,\boldsymbol{\Gamma}^k)$,

$$\omega_k=\frac{1}{M}\frac{\|\hat{\boldsymbol{D}}-\boldsymbol{D}^k\|^2}{\|F'(\boldsymbol{B}^k,\boldsymbol{\Gamma}^k)^T(\hat{\boldsymbol{D}}-\boldsymbol{D}^k)\|^2},$$

such that $M>1/2$ is chosen by the user [25]. We consider $M=N$.

Above, $\|\cdot\|$ denotes the Euclidean norm, and $F'(\boldsymbol{B}^k,\boldsymbol{\Gamma}^k)^T$ denotes the transpose of the Jacobian matrix of F computed at $(\boldsymbol{B}^k,\boldsymbol{\Gamma}^k)$. The above iteration is provably convergent under certain assumptions [25], and has the advantage that no matrix inversions are necessary. However, it requires the computation of F', a nontrivial task.

A theoretical result of this paper shows how to compute $F'(\boldsymbol{B}^k,\boldsymbol{\Gamma}^k)^T(\hat{\boldsymbol{D}}-\boldsymbol{D}^k)$ without explicitly computing $F'(\boldsymbol{B}^k,\boldsymbol{\Gamma}^k)^T$. We postpone the statement and the lengthy proof of this result to Section 4, but its application yields that

$$F'(\boldsymbol{B}^k,\boldsymbol{\Gamma}^k)^T(\hat{\boldsymbol{D}}\quad-\quad\boldsymbol{D}^k)\quad=\quad\left(\boldsymbol{\Upsilon}^T\widetilde{\boldsymbol{A}}^{k^T}\boldsymbol{M}^k\boldsymbol{A}^k+\widetilde{\boldsymbol{S}}_0^k-\widetilde{\boldsymbol{I}}_0^k\,,\;\boldsymbol{\Upsilon}^T\widetilde{\boldsymbol{A}}^{k^T}\boldsymbol{Q}\boldsymbol{A}^k+\widetilde{\boldsymbol{S}}_0^k-\widetilde{\boldsymbol{I}}_0^k\right). \tag{3.2}$$

The terms above are defined as follows. First, $\boldsymbol{A}^k$, $\boldsymbol{M}^k$ are defined as $\boldsymbol{A}$, $\boldsymbol{M}$ at the kth step of the iterative scheme. Next, consider the recurrence relation

$$\begin{cases}\widetilde{S}_j^k=\widetilde{S}_{j+1}^k-\beta_{j+1}^kI_{j+1}^k\widetilde{S}_{j+1}^k-\beta_{j+1}^kI_{j+1}^k\widetilde{I}_{j+1}^k+\hat{S}_{j+1}-S_{j+1}^k,\\ \widetilde{I}_j^k=\widetilde{I}_{j+1}^k+\beta_{j+1}^k\widetilde{I}_{j+1}^kS_{j+1}^k-\gamma_{j+1}^k\widetilde{I}_{j+1}^k+\beta_{j+1}^kS_{j+1}^k\widetilde{S}_{j+1}^k,\\ \widetilde{R}_j^k=\widetilde{R}_{j+1}^k+\gamma_{j+1}^k\widetilde{I}_{j+1}^k,\end{cases} \tag{3.3}$$

with final conditions $\widetilde{S}_N^k=0$, $\widetilde{I}_N^k=0$, $\widetilde{R}_N^k=0$, and define $\widetilde{\boldsymbol{A}}^k$ similarly to $\boldsymbol{A}$ but using $\widetilde{S}_j^k$, $\widetilde{I}_j^k$, $\widetilde{R}_j^k$ instead. Also,

$$\widetilde{\boldsymbol{S}}_0^k=\left(\widetilde{S}_0^k,\widetilde{S}_0^k,\ldots,\widetilde{S}_0^k\right)\in\mathbb{R}^N,\qquad\widetilde{\boldsymbol{I}}_0^k=\left(\widetilde{I}_0^k,\widetilde{I}_0^k,\ldots,\widetilde{I}_0^k\right)\in\mathbb{R}^N.$$

It follows from the iterative method (3.1) and identity (3.2) that

$$\boldsymbol{B}^{k+1}=\boldsymbol{B}^k-w^k\boldsymbol{\xi}^k,\qquad\boldsymbol{\Gamma}^{k+1}=\boldsymbol{\Gamma}^k+w^k\boldsymbol{\zeta}^k,\qquad w^k=\frac{1}{N}\frac{\|\boldsymbol{D}-\boldsymbol{D}^k\|^2}{\|(\boldsymbol{\xi}^k,\boldsymbol{\zeta}^k)\|^2}, \tag{3.4}$$

where we denote

$$\boldsymbol{\xi}^k=\boldsymbol{\Upsilon}^T\widetilde{\boldsymbol{A}}^{k^T}\boldsymbol{M}^k\boldsymbol{A}^k+\widetilde{\boldsymbol{S}}_0^k-\widetilde{\boldsymbol{I}}_0^k,\qquad\boldsymbol{\zeta}^k=\boldsymbol{\Upsilon}^T\widetilde{\boldsymbol{A}}^{k^T}\boldsymbol{Q}\boldsymbol{A}^k+\widetilde{\boldsymbol{S}}_0^k-\widetilde{\boldsymbol{I}}_0^k. \tag{3.5}$$

For given $\boldsymbol{B}^1$ and $\boldsymbol{\Gamma}^1$, the above steps completely describe the method. Indeed, from (3.3) we compute $\widetilde{\boldsymbol{A}}^k$ and then $\boldsymbol{\xi}^k$, $\boldsymbol{\zeta}^k$ follow from (3.5). That allows the computation of $\boldsymbol{B}^{k+1}$, $\boldsymbol{\Gamma}^{k+1}$ from (3.4).

It becomes clear from the numerical simulations that the algorithm performance was sensible to the initial guesses of $\boldsymbol{B}^1$ and $\boldsymbol{\Gamma}^1$. Approximating $\boldsymbol{\Gamma}$ from the data is usually easier since it depends on the recovering period of the infected patients. That does not hold for $\boldsymbol{B}$. To come up with a fair $\boldsymbol{B}^1$, we propose an preprocessing algorithm based on a SI (Susceptible-Infected) model.

The *SI* model is a simple compartmental models, written as

$$\hat{S}_{j+1} = \hat{S}_j - \frac{\beta_j^1 \hat{S}_j \hat{I}_j^{cumul}}{P}, \qquad \hat{I}_{j+1}^{cumul} = \hat{I}_j^{cumul} + \frac{\beta_j^1 \hat{S}_j \hat{I}_j^{cumul}}{P} \qquad \text{for } j = 1,\dots,N-1, \quad (3.6)$$

where we replace the susceptible and infected by the known data $\hat{\boldsymbol{S}}$ and $\hat{\boldsymbol{I}}$, leaving $\boldsymbol{B}^1$ as the only unknown. It follows from the first equation that

$$\beta_j^1 = -\frac{P\left(\hat{S}_{j+1} - \hat{S}_j\right)}{\hat{S}_j \hat{I}_j^{cumul}} \quad \text{for} \quad j = 1,2,\dots,N-1, \quad (3.7)$$

and we set $\beta_N^1 = \beta_{N-1}^1$. Note that the second equation in (3.6) is also satisfied since $\hat{S}_j = P - \hat{I}_j^{cumul}$.

For $\boldsymbol{\Gamma}^1$, we consider

$$\gamma_j^1 = 1/7, \qquad \text{for} \quad j = 1,2,\dots,N, \quad (3.8)$$

assuming that patients recover in week, in average.

As a way to measure the overall quality of our approximations and as a stopping criteria of our iterative scheme, we employ the regression (or determination) coefficient

$$R_2^k = 1 - \frac{\sum_{j=1}^{N} (\hat{S}_j - S_j^k)^2}{\sum_{j=1}^{N} (\hat{S}_j - \bar{\mathcal{S}})^2}, \qquad \bar{\mathcal{S}} = \frac{1}{N}\sum_{j=1}^{N} \hat{S}_j. \quad (3.9)$$

Such coefficient is often used to evaluate the fitting ability of various methods [7, 13, 16, 21, 27]. It ranges from zero to one, where being close to one indicates good approximations.

In this work, we stop our iterations as soon as $R_2^k > 0.99999$; See Algorithm 1.

4 APPLICATION OF THE MINIMUM ERROR METHOD TO THE MODEL

In this section, we show how to compute the action of the dual of F. Indeed, the following theorem holds.

Theorem 1. *Let F be described as above, where* (2.1) *holds. Then*

$$F'(\boldsymbol{B},\boldsymbol{\Gamma})^T(\hat{\boldsymbol{D}} - \boldsymbol{D}) = \left(\boldsymbol{\Upsilon}^T \widetilde{\boldsymbol{A}}^T \boldsymbol{M}\boldsymbol{A} + \widetilde{\boldsymbol{S}}_0 - \widetilde{\boldsymbol{I}}_0\,,\ \boldsymbol{\Upsilon}^T \widetilde{\boldsymbol{A}}^T \boldsymbol{Q}\boldsymbol{A} + \widetilde{\boldsymbol{S}}_0 - \widetilde{\boldsymbol{I}}_0\right),$$

Algorithm 1 Iteration to estimate $(\boldsymbol{B},\boldsymbol{\Gamma})$.

Data: $\hat{\boldsymbol{S}}$

Result: Compute an approximation for $(\boldsymbol{B},\boldsymbol{\Gamma})$ using the Minimal Error Iteration Scheme

Choose $(\boldsymbol{B}^1,\boldsymbol{\Gamma}^1)$ from Eqs. (3.7) and (3.8) Compute $\boldsymbol{S}^1$ and $\boldsymbol{I}^1$ from Eq. (1.1), up to $j=N-1$ replacing $(\boldsymbol{B},\boldsymbol{\Gamma})$ by $(\boldsymbol{B}^1,\boldsymbol{\Gamma}^1)$ Compute R_2^1 from Eq. (3.9), replacing $\boldsymbol{S}^k$ by $\boldsymbol{S}^1$ $k=1$ **while** $\left(R_2^k<0.99999\right)$ **do**

  Compute $\boldsymbol{s}^{k+1}$ and $\boldsymbol{i}^{k+1}$ from Eq. (3.3), replacing $(\boldsymbol{B}^k,\boldsymbol{\Gamma}^k)$ by $(\boldsymbol{B}^{k+1},\boldsymbol{\Gamma}^{k+1})$ Compute $(\boldsymbol{B}^{k+1},\boldsymbol{\Gamma}^{k+1})$ using Eq. (3.4) Compute $\boldsymbol{S}^{k+1}$ and $\boldsymbol{I}^{k+1}$ from Eq. (1.1), replacing $(\boldsymbol{B},\boldsymbol{\Gamma})$ by $(\boldsymbol{B}^{k+1},\boldsymbol{\Gamma}^{k+1})$ Compute R_2^{k+1} from Eq (3.9), replacing $\boldsymbol{S}^k$ by $\boldsymbol{S}^{k+1}$ k=k+1;

end

where we define $\widetilde{\boldsymbol{A}}$, $\widetilde{\boldsymbol{S}}_0$, $\widetilde{\boldsymbol{I}}_0$ *as follows. Consider first the recurrence relation*

$$\begin{cases}\widetilde{S}_j=\widetilde{S}_{j+1}-\beta_{j+1}I_{j+1}\widetilde{S}_{j+1}-\beta_{j+1}I_{j+1}\widetilde{I}_{j+1}+\hat{S}_{j+1}-S_{j+1},\\ \widetilde{I}_j=\widetilde{I}_{j+1}+\beta_{j+1}\widetilde{I}_{j+1}S_{j+1}-\gamma_{j+1}\widetilde{I}_{j+1}+\beta_{j+1}S_{j+1}\widetilde{S}_{j+1},\\ \widetilde{R}_j=\widetilde{R}_{j+1}+\gamma_{j+1}\widetilde{I}_{j+1},\end{cases}$$

with final conditions $\widetilde{S}_N=0$, $\widetilde{I}_N=0$, $\widetilde{R}_N=0$, *and define* $\widetilde{\boldsymbol{A}}$ *as* $\boldsymbol{A}$ *but using* $\widetilde{S}_j$, $\widetilde{I}_j$, $\widetilde{R}_j$. *Let,*

$$\widetilde{\boldsymbol{S}}_0=\left(\widetilde{S}_0,\widetilde{S}_0,\ldots,\widetilde{S}_0\right)\in\mathbb{R}^N,\qquad \widetilde{\boldsymbol{I}}_0=\left(\widetilde{I}_0,\widetilde{I}_0,\ldots,\widetilde{I}_0\right)\in\mathbb{R}^N.$$

Proof. Let $F(\boldsymbol{x})=\boldsymbol{D}$, where $\boldsymbol{x}=(\boldsymbol{B},\boldsymbol{\Gamma})$ and $\boldsymbol{D}$ is such that (2.1) holds. Let $\boldsymbol{\Theta_B}=(\theta_{\beta_1},\theta_{\beta_2},\ldots,\theta_{\beta_N})$, $\boldsymbol{\Theta_\Gamma}=(\theta_{\gamma_1},\theta_{\gamma_2},\ldots,\theta_{\gamma_N})$, $\boldsymbol{\Theta}=(\boldsymbol{\Theta_B},\boldsymbol{\Theta_\Gamma})\in\mathbb{R}^{2N}$ be arbitrary vectors, and $\lambda\in\mathbb{R}$ be nonzero. Evaluating the operator F at $\boldsymbol{x}+\lambda\boldsymbol{\Theta}$, we obtain $F(\boldsymbol{x}+\lambda\boldsymbol{\Theta})=\boldsymbol{D}^\lambda$, where $\boldsymbol{D}^\lambda$ is such that

$$\begin{cases}S_{j+1}^\lambda=S_j^\lambda-\left(\beta_j+\lambda\theta_{\beta_j}\right)I_j^\lambda S_j^\lambda,\\ I_{j+1}^\lambda=I_j^\lambda+\left(\beta_j+\lambda\theta_{\beta_j}\right)I_j^\lambda S_j^\lambda-\left(\gamma_j+\lambda\theta_{\gamma_j}\right)I_j^\lambda,\\ R_{j+1}^\lambda=R_j^\lambda+\left(\gamma_j+\lambda\theta_{\gamma_j}\right)I_j^\lambda,\\ S_1^\lambda=S_1+\lambda\sum_{j=1}^N\left(\theta_{\beta_j}+\theta_{\gamma_j}\right),\\ I_1^\lambda=1-S_1-\lambda\sum_{j=1}^N\left(\theta_{\beta_j}+\theta_{\gamma_j}\right),\\ R_1^\lambda=0.\end{cases}\tag{4.1}$$

As in (2.1), we gather that

$$\boldsymbol{\Lambda}^\lambda\boldsymbol{\Upsilon}=\boldsymbol{A}^\lambda\boldsymbol{\Upsilon}+\boldsymbol{M}^\lambda\boldsymbol{A}^\lambda(\boldsymbol{B}^\lambda+\lambda\boldsymbol{\Theta_B})+\boldsymbol{Q}\boldsymbol{A}^\lambda(\boldsymbol{\Gamma}^\lambda+\lambda\boldsymbol{\Theta_\Gamma}),\tag{4.2}$$

with initial condition

$$\boldsymbol{a}_1^\lambda=\left(S(1)+\left\langle(\boldsymbol{\Upsilon},\boldsymbol{\Upsilon}),(\boldsymbol{\Theta_B},\boldsymbol{\Theta_\Gamma})\right\rangle_{\mathbb{R}^{2N}},1-S(1)-\left\langle(\boldsymbol{\Upsilon},\boldsymbol{\Upsilon})\,,\,(\boldsymbol{\Theta_B},\boldsymbol{\Theta_\Gamma})\right\rangle_{\mathbb{R}^{2N}}\,,\,0\right).$$

The Gateaux derivative of F at $\boldsymbol{x}$ in the direction $\boldsymbol{\Theta}$ is given by

$$\overline{\boldsymbol{D}} = F'(\boldsymbol{x})(\boldsymbol{\Theta}) = \lim_{\lambda\to 0} \frac{F(\boldsymbol{x}+\lambda\boldsymbol{\Theta}) - F(\boldsymbol{x})}{\lambda}, \tag{4.3}$$

where $\overline{\boldsymbol{D}} = (\bar{S}_1, 0, 0, \bar{S}_2, 0, 0, \ldots, \bar{S}_N, 0, 0)$. We denote the following limits

$$\overline{\boldsymbol{A}} = \lim_{\lambda\to 0} \frac{\boldsymbol{A}^\lambda - \boldsymbol{A}}{\lambda}, \qquad \overline{\boldsymbol{\Lambda}} = \lim_{\lambda\to 0} \frac{\boldsymbol{\Lambda}^\lambda - \boldsymbol{\Lambda}}{\lambda}, \qquad \overline{\boldsymbol{M}} = \lim_{\lambda\to 0} \frac{\boldsymbol{M}^\lambda - \boldsymbol{M}}{\lambda}. \tag{4.4}$$

Considering the difference between (4.2) and (2.1), dividing by λ and taking the limit $\lambda \to 0$, we have

$$\overline{\boldsymbol{\Lambda}}\boldsymbol{\Upsilon} = \overline{\boldsymbol{A}}\boldsymbol{\Upsilon} + \overline{\boldsymbol{M}}\boldsymbol{A}\boldsymbol{B} + \boldsymbol{M}\overline{\boldsymbol{A}}\boldsymbol{B} + \boldsymbol{M}\boldsymbol{A}\Theta_{\boldsymbol{B}} + \boldsymbol{Q}\overline{\boldsymbol{A}}\boldsymbol{\Gamma} + \boldsymbol{Q}\boldsymbol{A}\Theta_{\boldsymbol{\Gamma}}, \tag{4.5}$$

with initial condition

$$\bar{\boldsymbol{a}}_1 = \left(\left\langle (\boldsymbol{\Upsilon}, \boldsymbol{\Upsilon}), (\boldsymbol{\Theta}_{\boldsymbol{B}}, \boldsymbol{\Theta}_{\boldsymbol{\Gamma}}) \right\rangle_{\mathbb{R}^{2N}}, -\left\langle (\boldsymbol{\Upsilon}, \boldsymbol{\Upsilon}) \, , \, (\boldsymbol{\Theta}_{\boldsymbol{B}}, \boldsymbol{\Theta}_{\boldsymbol{\Gamma}}) \right\rangle_{\mathbb{R}^{2N}} , \, 0 \right).$$

This last equation is yet another system of coupled nonlinear difference equations, depending on the parameter $\boldsymbol{\Theta}$, representing an arbitrary point in $\mathbb{R}^{2N}$. From the minimal error iteration (3.1) and $\boldsymbol{\Theta} \in \mathbb{R}^{2N}$ arbitrary, we have

$$\left\langle F'(\boldsymbol{x})^T(\hat{\boldsymbol{D}} - F(\boldsymbol{x})), \boldsymbol{\Theta} \right\rangle_{\mathbb{R}^{2N}} = \left\langle F'(\boldsymbol{x})^T(\hat{\boldsymbol{D}} - \boldsymbol{D}), \boldsymbol{\Theta} \right\rangle_{\mathbb{R}^{2N}} = \left\langle \hat{\boldsymbol{D}} - \boldsymbol{D}, \, F'(\boldsymbol{x})(\boldsymbol{\Theta}) \right\rangle_{\mathbb{R}^{3N}}.$$

by definition of adjoint operator. From Eq. (4.3) and the previous equation, we obtain

$$\left\langle F'(\boldsymbol{x})^T(\hat{\boldsymbol{D}} - F(\boldsymbol{x})), \boldsymbol{\Theta} \right\rangle_{\mathbb{R}^{2N}} = \left\langle \hat{\boldsymbol{D}} - \boldsymbol{D}, \, \overline{\boldsymbol{D}} \right\rangle_{\mathbb{R}^{3N}} = \left\langle \hat{\boldsymbol{D}} - \boldsymbol{D}, \, \overline{\boldsymbol{A}} \right\rangle_{\mathbb{R}^{3N}}, \tag{4.6}$$

Multiplying (4.5) by $\widetilde{\boldsymbol{A}}^T$, we obtain

$$\begin{aligned} \boldsymbol{\Upsilon}^T\widetilde{\boldsymbol{A}}\overline{\boldsymbol{\Lambda}}\boldsymbol{\Upsilon} = \boldsymbol{\Upsilon}^T\widetilde{\boldsymbol{A}}^T\overline{\boldsymbol{A}}\boldsymbol{\Upsilon} + \boldsymbol{\Upsilon}^T\widetilde{\boldsymbol{A}}^T\overline{\boldsymbol{M}}\boldsymbol{A}\boldsymbol{B} + \boldsymbol{\Upsilon}^T\widetilde{\boldsymbol{A}}^T\boldsymbol{M}\overline{\boldsymbol{A}}\boldsymbol{B} + \\ \boldsymbol{\Upsilon}^T\widetilde{\boldsymbol{A}}^T\boldsymbol{M}\boldsymbol{A}\Theta_{\boldsymbol{B}} + \boldsymbol{\Upsilon}^T\widetilde{\boldsymbol{A}}^T\boldsymbol{Q}\overline{\boldsymbol{A}}\boldsymbol{\Gamma} + \boldsymbol{\Upsilon}^T\widetilde{\boldsymbol{A}}^T\boldsymbol{Q}\boldsymbol{A}\Theta_{\boldsymbol{\Gamma}}. \end{aligned} \tag{4.7}$$

We denote

$$\widetilde{\boldsymbol{\Lambda}} = \begin{pmatrix} \widetilde{\boldsymbol{a}}_0 & \boldsymbol{o} & \ldots & \boldsymbol{o} \\ \boldsymbol{o} & \widetilde{\boldsymbol{a}}_1 & \ldots & \boldsymbol{o} \\ \boldsymbol{o} & \boldsymbol{o} & \ldots & \boldsymbol{o} \\ \vdots & \vdots & \ddots & \vdots \\ \boldsymbol{o} & \boldsymbol{o} & \ldots & \widetilde{\boldsymbol{a}}_N \end{pmatrix}$$

then, from (3.3), we have

$$\widetilde{\boldsymbol{\Lambda}}\boldsymbol{\Upsilon} = \widetilde{\boldsymbol{A}}\boldsymbol{\Upsilon} + \widetilde{\boldsymbol{M}}\boldsymbol{A}\boldsymbol{B} - \boldsymbol{M}^T\widetilde{\boldsymbol{A}}\boldsymbol{B} + \boldsymbol{Q}^T\widetilde{\boldsymbol{A}}\boldsymbol{\Gamma} + \hat{\boldsymbol{D}} - \boldsymbol{D}. \tag{4.8}$$

Multiplying (4.8) by $\overline{\boldsymbol{A}}^T$, it follows that

$$\boldsymbol{\Upsilon}^T\overline{\boldsymbol{A}}^T\widetilde{\boldsymbol{\Lambda}}\boldsymbol{\Upsilon} = \boldsymbol{\Upsilon}^T\overline{\boldsymbol{A}}^T\widetilde{\boldsymbol{A}}\boldsymbol{\Upsilon} + \boldsymbol{\Upsilon}^T\overline{\boldsymbol{A}}^T\widetilde{\boldsymbol{M}}\boldsymbol{A}\boldsymbol{B} - \boldsymbol{\Upsilon}^T\overline{\boldsymbol{A}}^T\boldsymbol{M}^T\widetilde{\boldsymbol{A}}\boldsymbol{B} + \boldsymbol{\Upsilon}^T\overline{\boldsymbol{A}}^T\boldsymbol{Q}^T\widetilde{\boldsymbol{A}}\boldsymbol{\Gamma} + \boldsymbol{\Upsilon}^T\overline{\boldsymbol{A}}^T(\hat{\boldsymbol{D}} - \boldsymbol{D}). \tag{4.9}$$

Note that

$$\begin{aligned} &\bar{\boldsymbol{A}}^T\widetilde{\boldsymbol{A}} = \widetilde{\boldsymbol{A}}^T\bar{\boldsymbol{A}}, \qquad \bar{\boldsymbol{A}}^T\widetilde{\boldsymbol{M}} = \widetilde{\boldsymbol{A}}^T\overline{\boldsymbol{M}}, \qquad -\bar{\boldsymbol{A}}^T\boldsymbol{M}^T\widetilde{\boldsymbol{A}} = \widetilde{\boldsymbol{A}}^T\boldsymbol{M}\bar{\boldsymbol{A}} \\ &\bar{\boldsymbol{A}}^T\boldsymbol{Q}^T\widetilde{\boldsymbol{A}} = \widetilde{\boldsymbol{A}}^T\boldsymbol{Q}\bar{\boldsymbol{A}}, \qquad \bar{\boldsymbol{A}}^T\boldsymbol{Q}^T\widetilde{\boldsymbol{A}} = \widetilde{\boldsymbol{A}}^T\boldsymbol{Q}\bar{\boldsymbol{A}}. \end{aligned} \tag{4.10}$$

Substituting (4.10) in (4.9), we have

$$\boldsymbol{\Upsilon}^T\bar{\boldsymbol{A}}^T\widetilde{\boldsymbol{\Lambda}}\boldsymbol{\Upsilon} = \boldsymbol{\Upsilon}^T\widetilde{\boldsymbol{A}}^T\bar{\boldsymbol{A}}\boldsymbol{\Upsilon} + \boldsymbol{\Upsilon}^T\widetilde{\boldsymbol{A}}^T\overline{\boldsymbol{M}}\boldsymbol{A}\boldsymbol{B} + \boldsymbol{\Upsilon}^T\widetilde{\boldsymbol{A}}^T\boldsymbol{M}\bar{\boldsymbol{A}}\boldsymbol{B} + \boldsymbol{\Upsilon}^T\widetilde{\boldsymbol{A}}^T\boldsymbol{Q}\bar{\boldsymbol{A}}\boldsymbol{\Gamma} + \boldsymbol{\Upsilon}^T\bar{\boldsymbol{A}}^T(\hat{\boldsymbol{D}} - \boldsymbol{D}). \tag{4.11}$$

Subtracting equations (4.7) and (4.11),

$$\begin{aligned} \boldsymbol{\Upsilon}^T\widetilde{\boldsymbol{A}}^T\bar{\boldsymbol{\Lambda}}\boldsymbol{\Upsilon} - \boldsymbol{\Upsilon}^T\bar{\boldsymbol{A}}^T\widetilde{\boldsymbol{\Lambda}}\boldsymbol{\Upsilon} &= \boldsymbol{\Upsilon}^T\widetilde{\boldsymbol{A}}^T\boldsymbol{M}\boldsymbol{A}\boldsymbol{\Theta}_{\boldsymbol{B}} + \boldsymbol{\Upsilon}^T\widetilde{\boldsymbol{A}}^T\boldsymbol{Q}\boldsymbol{A}\boldsymbol{\Theta}_{\boldsymbol{\Gamma}} - \boldsymbol{\Upsilon}^T\bar{\boldsymbol{A}}^T(\hat{\boldsymbol{D}} - \boldsymbol{D}) \\ \widetilde{\boldsymbol{a}}_N^T\bar{\boldsymbol{a}}_{N+1} - \bar{\boldsymbol{a}}_1^T\widetilde{\boldsymbol{a}}_0 &= \boldsymbol{\Upsilon}^T\widetilde{\boldsymbol{A}}^T\boldsymbol{M}\boldsymbol{A}\boldsymbol{\Theta}_{\boldsymbol{B}} + \boldsymbol{\Upsilon}^T\widetilde{\boldsymbol{A}}^T\boldsymbol{Q}\boldsymbol{A}\boldsymbol{\Theta}_{\boldsymbol{\Gamma}} - \boldsymbol{\Upsilon}^T\bar{\boldsymbol{A}}^T(\hat{\boldsymbol{D}} - \boldsymbol{D}). \end{aligned}$$

From (3.3), $\widetilde{\boldsymbol{a}}_N^T = (0,0,0)$, and previous equation, we gather that

$$\begin{aligned} -\bar{\boldsymbol{a}}_1^T\widetilde{\boldsymbol{a}}_0 &= \left\langle \boldsymbol{\Upsilon}^T\widetilde{\boldsymbol{A}}^T\boldsymbol{M}\boldsymbol{A}, \boldsymbol{\Theta}_{\boldsymbol{B}} \right\rangle_{\mathbb{R}^N} + \left\langle \boldsymbol{\Upsilon}^T\widetilde{\boldsymbol{A}}^T\boldsymbol{Q}\boldsymbol{A}, \boldsymbol{\Theta}_{\boldsymbol{\Gamma}} \right\rangle_{\mathbb{R}^N} - \left\langle \hat{\boldsymbol{D}} - \boldsymbol{D},\ \boldsymbol{\Upsilon}^T\bar{\boldsymbol{A}} \right\rangle_{\mathbb{R}^{3N}} \\ &= \left\langle \left(\widetilde{\boldsymbol{A}}^T\boldsymbol{M}\boldsymbol{A}, \widetilde{\boldsymbol{A}}^T\boldsymbol{Q}\boldsymbol{A}\right), (\boldsymbol{\Theta}_{\boldsymbol{B}}, \boldsymbol{\Theta}_{\boldsymbol{\Gamma}}) \right\rangle_{\mathbb{R}^{2N}} - \left\langle \hat{\boldsymbol{D}} - \boldsymbol{D},\ \boldsymbol{\Upsilon}^T\bar{\boldsymbol{A}} \right\rangle_{\mathbb{R}^{3N}}. \end{aligned}$$

So we have

$$\left\langle \hat{\boldsymbol{D}} - \boldsymbol{D},\ \bar{\boldsymbol{A}}\boldsymbol{\Upsilon} \right\rangle_{\mathbb{R}^{3N}} = \left\langle \left(\boldsymbol{\Upsilon}^T\widetilde{\boldsymbol{A}}^T\boldsymbol{M}\boldsymbol{A}, \boldsymbol{\Upsilon}^T\widetilde{\boldsymbol{A}}^T\boldsymbol{Q}\boldsymbol{A}\right), (\boldsymbol{\Theta}_{\boldsymbol{B}}, \boldsymbol{\Theta}_{\boldsymbol{\Gamma}}) \right\rangle_{\mathbb{R}^{2N}} + \bar{\boldsymbol{a}}_1^T\widetilde{\boldsymbol{a}}_0.$$

From equation (4.5) and the previous equation, we obtain

$$\begin{aligned} \left\langle \hat{\boldsymbol{D}} - \boldsymbol{D},\ \bar{\boldsymbol{A}}\boldsymbol{\Upsilon} \right\rangle_{\mathbb{R}^{3N}} = &\left\langle \left(\boldsymbol{\Upsilon}^T\widetilde{\boldsymbol{A}}^T\boldsymbol{M}\boldsymbol{A}, \boldsymbol{\Upsilon}^T\widetilde{\boldsymbol{A}}^T\boldsymbol{Q}\boldsymbol{A}\right), (\boldsymbol{\Theta}_{\boldsymbol{B}}, \boldsymbol{\Theta}_{\boldsymbol{\Gamma}}) \right\rangle \\ &+ \left(\left\langle (\boldsymbol{\Upsilon}, \boldsymbol{\Upsilon}), (\boldsymbol{\Theta}_{\boldsymbol{B}}, \boldsymbol{\Theta}_{\boldsymbol{\Gamma}}) \right\rangle, -\left\langle (\boldsymbol{\Upsilon}, \boldsymbol{\Upsilon})\ ,\ (\boldsymbol{\Theta}_{\boldsymbol{B}}, \boldsymbol{\Theta}_{\boldsymbol{\Gamma}}) \right\rangle\ ,\ 0 \right) \left(\widetilde{S}_0, \widetilde{I}_0, \widetilde{R}_0\right)^T. \end{aligned}$$

Then

$$\begin{aligned} \left\langle \hat{\boldsymbol{D}} - \boldsymbol{D},\ \bar{\boldsymbol{A}} \right\rangle_{\mathbb{R}^{3N}} &= \left\langle \left(\boldsymbol{\Upsilon}^T\widetilde{\boldsymbol{A}}^T\boldsymbol{M}\boldsymbol{A}, \boldsymbol{\Upsilon}^T\widetilde{\boldsymbol{A}}^T\boldsymbol{Q}\boldsymbol{A}\right), (\boldsymbol{\Theta}_{\boldsymbol{B}}, \boldsymbol{\Theta}_{\boldsymbol{\Gamma}}) \right\rangle \\ &\quad + \left\langle (\widetilde{\boldsymbol{S}}_0, \widetilde{\boldsymbol{S}}_0), (\boldsymbol{\Theta}_{\boldsymbol{B}}, \boldsymbol{\Theta}_{\boldsymbol{\Gamma}}) \right\rangle - \left\langle (\widetilde{\boldsymbol{I}}_0, \widetilde{\boldsymbol{I}}_0)\ ,\ (\boldsymbol{\Theta}_{\boldsymbol{B}}, \boldsymbol{\Theta}_{\boldsymbol{\Gamma}}) \right\rangle \\ &= \left\langle \left(\boldsymbol{\Upsilon}^T\widetilde{\boldsymbol{A}}^T\boldsymbol{M}\boldsymbol{A} + \widetilde{\boldsymbol{S}}_0 - \widetilde{\boldsymbol{I}}_0\ ,\ \boldsymbol{\Upsilon}^T\widetilde{\boldsymbol{A}}^T\boldsymbol{Q}\boldsymbol{A} + \widetilde{\boldsymbol{S}}_0 - \widetilde{\boldsymbol{I}}_0\right)\ ,\ (\boldsymbol{\Theta}_{\boldsymbol{B}}, \boldsymbol{\Theta}_{\boldsymbol{\Gamma}}) \right\rangle_{\mathbb{R}^{2N}}. \end{aligned} \tag{4.12}$$

From Eqs. (4.12) and (4.6)

$$\begin{aligned} &\left\langle F'(\boldsymbol{x})^T(\hat{\boldsymbol{D}} - F(\boldsymbol{x})), \boldsymbol{\Theta} \right\rangle_{\mathbb{R}^{2N}} = \\ &\qquad \left\langle \left(\boldsymbol{\Upsilon}^T\widetilde{\boldsymbol{A}}^T\boldsymbol{M}\boldsymbol{A} + \widetilde{\boldsymbol{S}}_0 - \widetilde{\boldsymbol{I}}_0\ ,\ \boldsymbol{\Upsilon}^T\widetilde{\boldsymbol{A}}^T\boldsymbol{Q}\boldsymbol{A} + \widetilde{\boldsymbol{S}}_0 - \widetilde{\boldsymbol{I}}_0\right)\ ,\ (\boldsymbol{\Theta}_{\boldsymbol{B}}, \boldsymbol{\Theta}_{\boldsymbol{\Gamma}}) \right\rangle_{\mathbb{R}^{2N}}. \end{aligned}$$

Since $\boldsymbol{\Theta} \in \mathbb{R}^{2N}$ is arbitrary, we obtain

$$F'(\boldsymbol{x}^k)^T(\hat{\boldsymbol{D}} - F(\boldsymbol{x})) = \left(\boldsymbol{\Upsilon}^T\widetilde{\boldsymbol{A}}^T\boldsymbol{M}\boldsymbol{A} + \widetilde{\boldsymbol{S}}_0 - \widetilde{\boldsymbol{I}}_0\,,\ \boldsymbol{\Upsilon}^T\widetilde{\boldsymbol{A}}^T\boldsymbol{Q}\boldsymbol{A} + \widetilde{\boldsymbol{S}}_0 - \widetilde{\boldsymbol{I}}_0\right).$$

□

5 NUMERICAL RESULTS

We consider numerical results for the evolution of the COVID-19 pandemics using data from two cities in Brazil: Rio de Janeiro, with a total population of 6.775.561 people, and the city of Petrópolis, with a population of "only" 307.144 people. The epidemiological data was obtained from the Brazilian Ministry of Health (`https://covid.saude.gov.br`), for the period March 28, 2020 up to February 10, 2021, when the Brazilian Government started vaccination campaigns. Due to the EMA-smoothing procedure of the data, we consider for practical purposes that the available data starts on April 03, 2020.

Using the minimal error method, implemented as in Algorithm 1, we estimate the time-dependent transmission probability $\boldsymbol{B}$ and removal probability $\boldsymbol{\Gamma}$, using as data the susceptible population $\hat{\boldsymbol{S}}$. In the process, we also estimate $\boldsymbol{R}$, the size of the immune population at a certain given moment, and $\boldsymbol{I}$, the total number of infected people. Note that $\boldsymbol{I}$ cannot be obtained directly from $\hat{\boldsymbol{I}}^{cumul}$ since this later data refer to the total amount of infected patients since the start of the pandemic, and $\boldsymbol{I}$ is related to the total amount of sick patients at a fixed day. Knowing $\boldsymbol{B}$ and $\boldsymbol{\Gamma}$, we compute the discrete-time basic and effective reproduction numbers

$$\mathcal{R}_j^\circ = \frac{\beta_j}{\gamma_j}, \qquad \mathcal{R}_j = \frac{\beta_j}{\gamma_j}S_j = \mathcal{R}_j^\circ S_j \qquad j = 1,2,\cdots,N,$$

and $\boldsymbol{\mathcal{R}}^\circ = (\mathcal{R}_1^\circ, \mathcal{R}_2^\circ, \ldots, \mathcal{R}_N^\circ)$, $\boldsymbol{\mathcal{R}} = (\mathcal{R}_1, \mathcal{R}_2, \ldots, \mathcal{R}_N)$.

We start by showing that the smoothing step preserves accuracy while smoothing the data. Figure 1, displays $\hat{\boldsymbol{I}}^{\mathrm{EMA}}$ and $\hat{\boldsymbol{I}}^{cumul}$ for the cities of Rio de Janeiro and Petrópolis. Note that $\hat{\boldsymbol{I}}^{\mathrm{EMA}}$ is able to smooth out the rough data.

Next we show the numerical results related to our scheme. The data estimation for the final days suffer from a minor instability, and to avoid that we disregard the last five days from the data.

Figure 2 presents the results obtained from the SIR model (1.1) using the estimated parameters $\boldsymbol{B}$ and $\boldsymbol{\Gamma}$. Subplot (A) compares the susceptible population real data (in red) with the model results (in blue). Note that are no perceptive difference between data and our computer simulation, showing that our parameter estimation algorithm is effective. Subplots (B) and (C) represent the infected and removed population obtained from the SIR model. See also Figure 4 for similar results for Petrópolis.

Figure 3-A displays the estimated infection and recovery probability parameters. We point out that the recovery probability is roughly $1/10$, very similar to what is used for numerical simulations. Figure 3-B shows the computed basic and effective reproduction numbers. Finally,

Figure 3-C shows the number of new reported cases. Note that running SIR model with the estimated parameters yields an accurate aproximation of the smoothed data.

The results for Petrópolis are similar (see Figures 4 and 5) indicating that the method also works for cities with smaller populations.

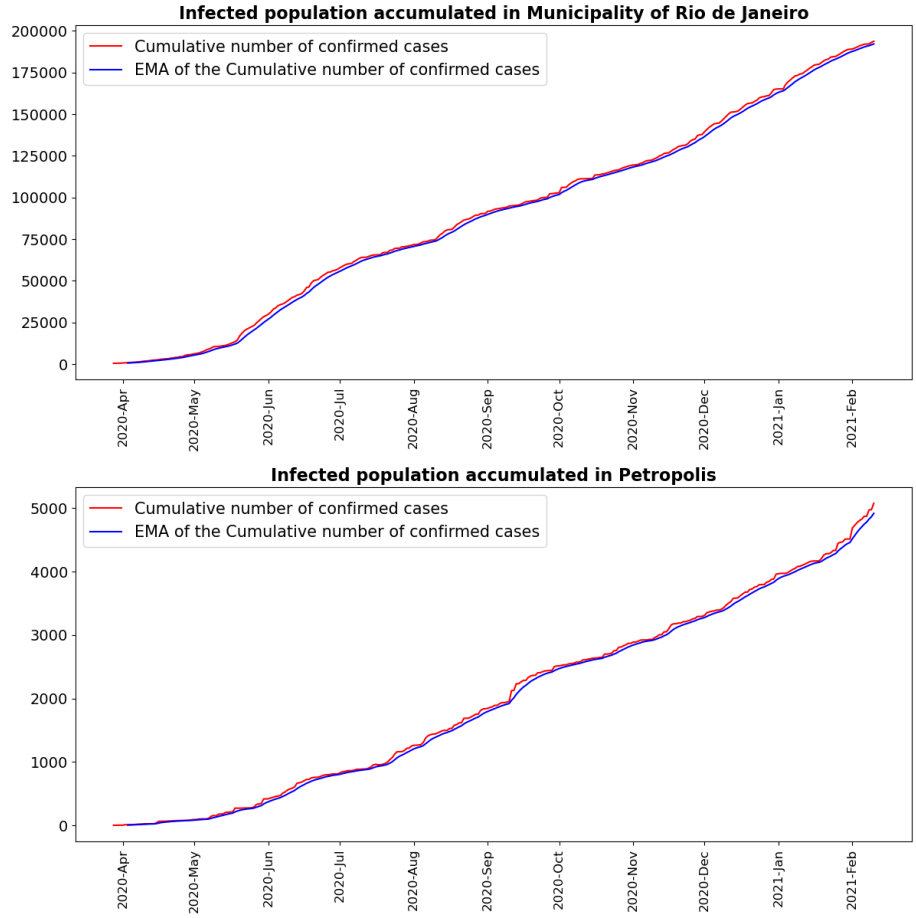

Figure 1: Plots for Rio de Janeiro and Petrópolis. The red line represents the cumulative number of confirmed cases from March 28, 2020, to February 10, 2021. The blue line is the EMA of the cumulative number of confirmed cases from April 03, 2020, to February 10, 2021.

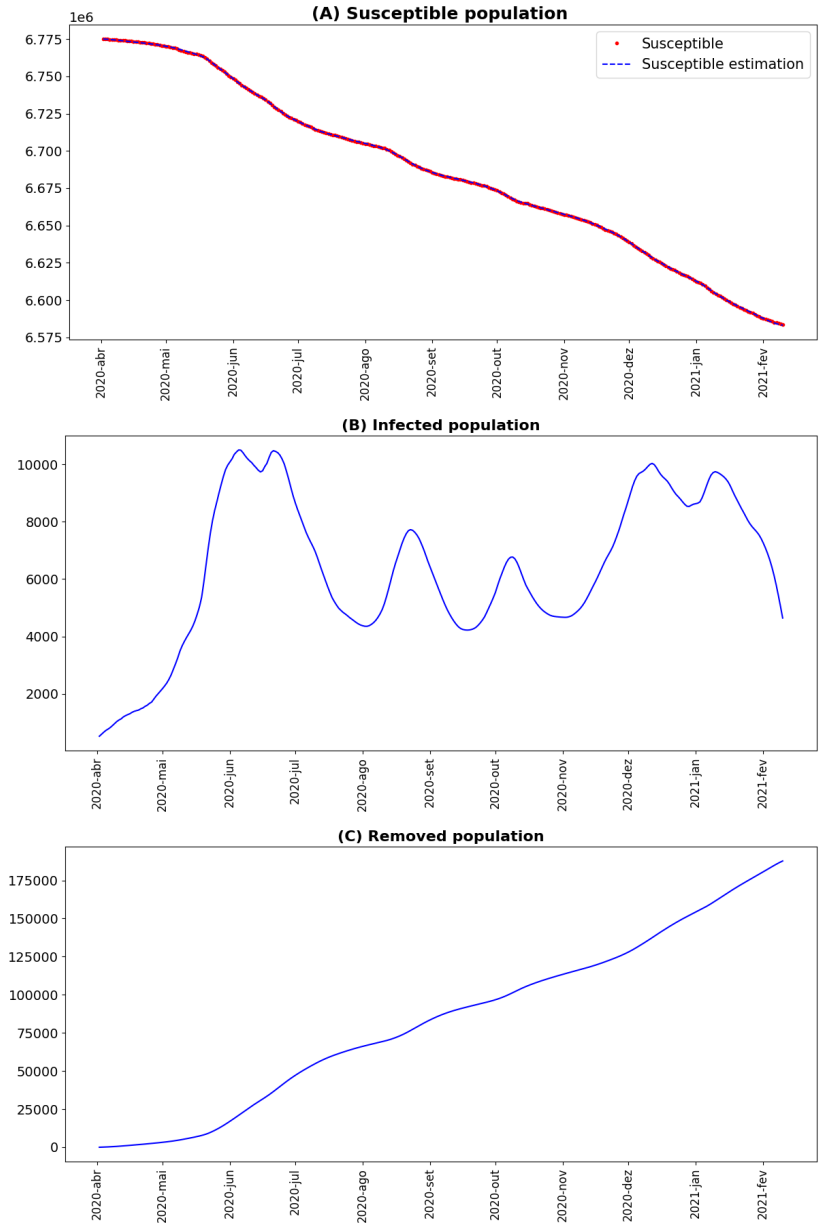

Figure 2: Plots for Rio de Janeiro. The y-axis represents the population. Subplot (A) shows the susceptible population, where the red line is the real data and the blue line is the approximation obtained from the SIR model (1.1) using the estimated parameters. Subplots (B) and (C) represent the infected and removed population obtained from the SIR model, respectively.

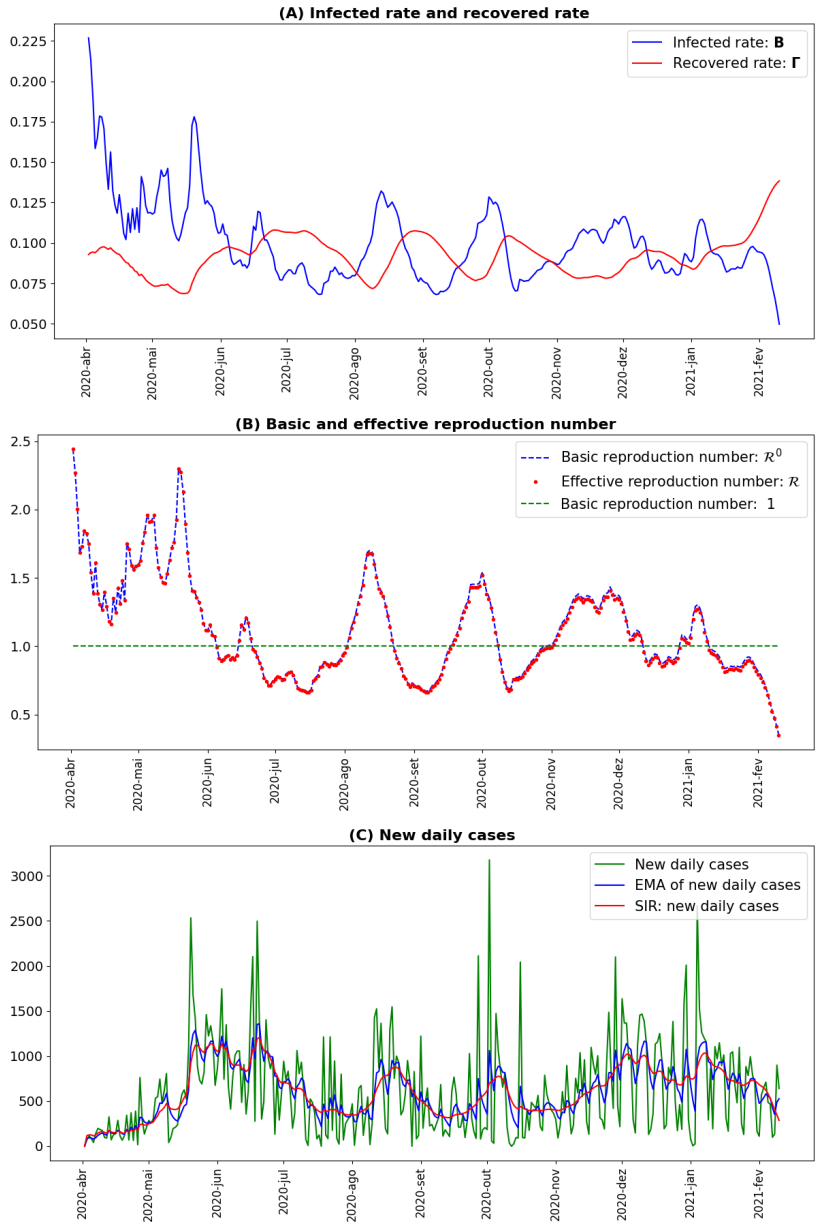

Figure 3: Plots for Rio de Janeiro. In Subplot (A), the blue line represents the transmission probability and red line shows the removal probability. Subplot (B) displays the basic and effective reproduction numbers (we also plot the constant line equal to one as a reference). In Subplot (C), the green line represents the new daily cases from March 28, 2020, to February 10, 2021. The blue line is the EMA of the new daily cases from April 03, 2020, to February 10, 2021. The red plot depicts the predicted new cases using the estimated parameters.

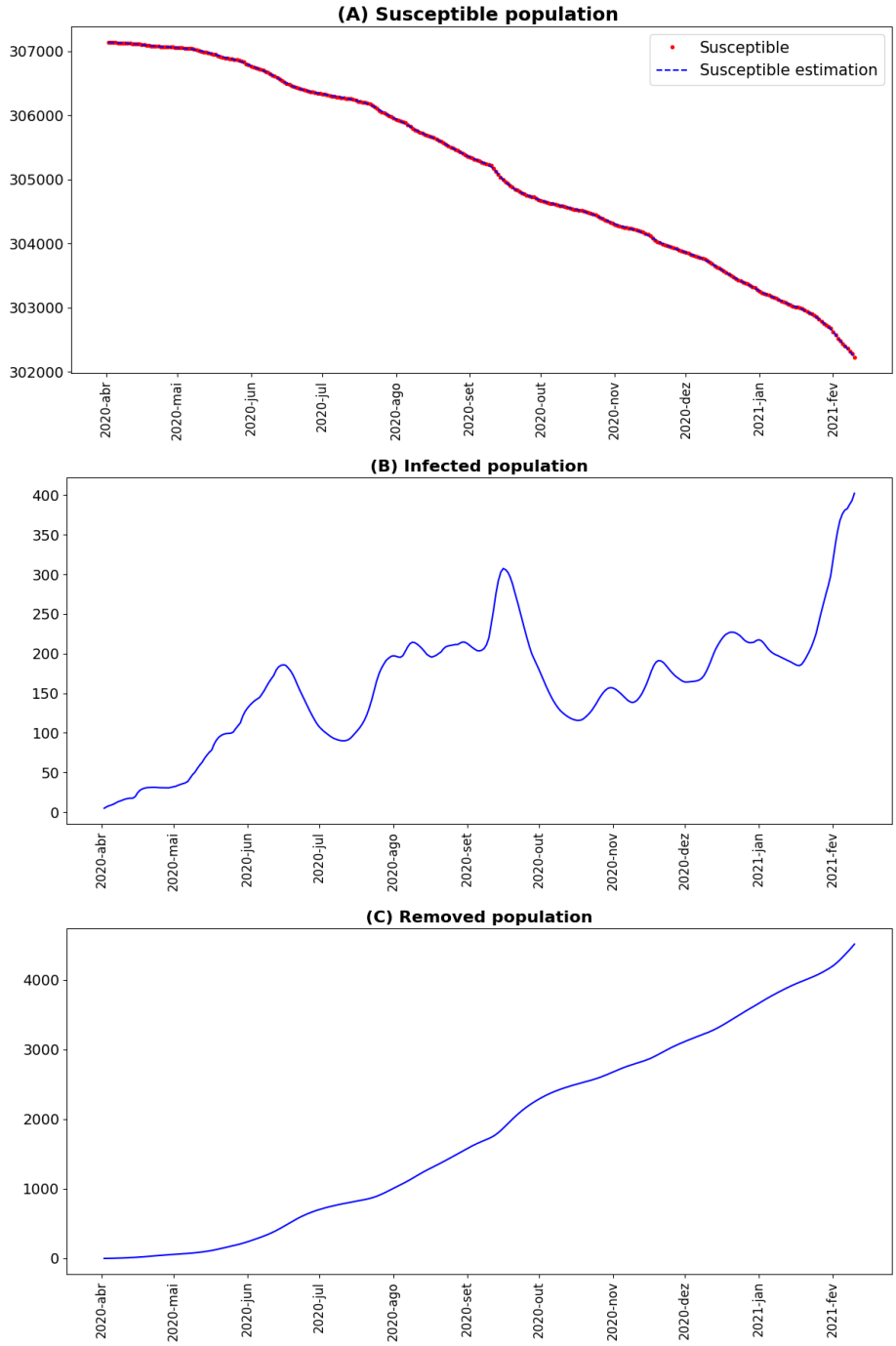

Figure 4: Plots for Petrópolis. See Figure 2 for the subplot description.

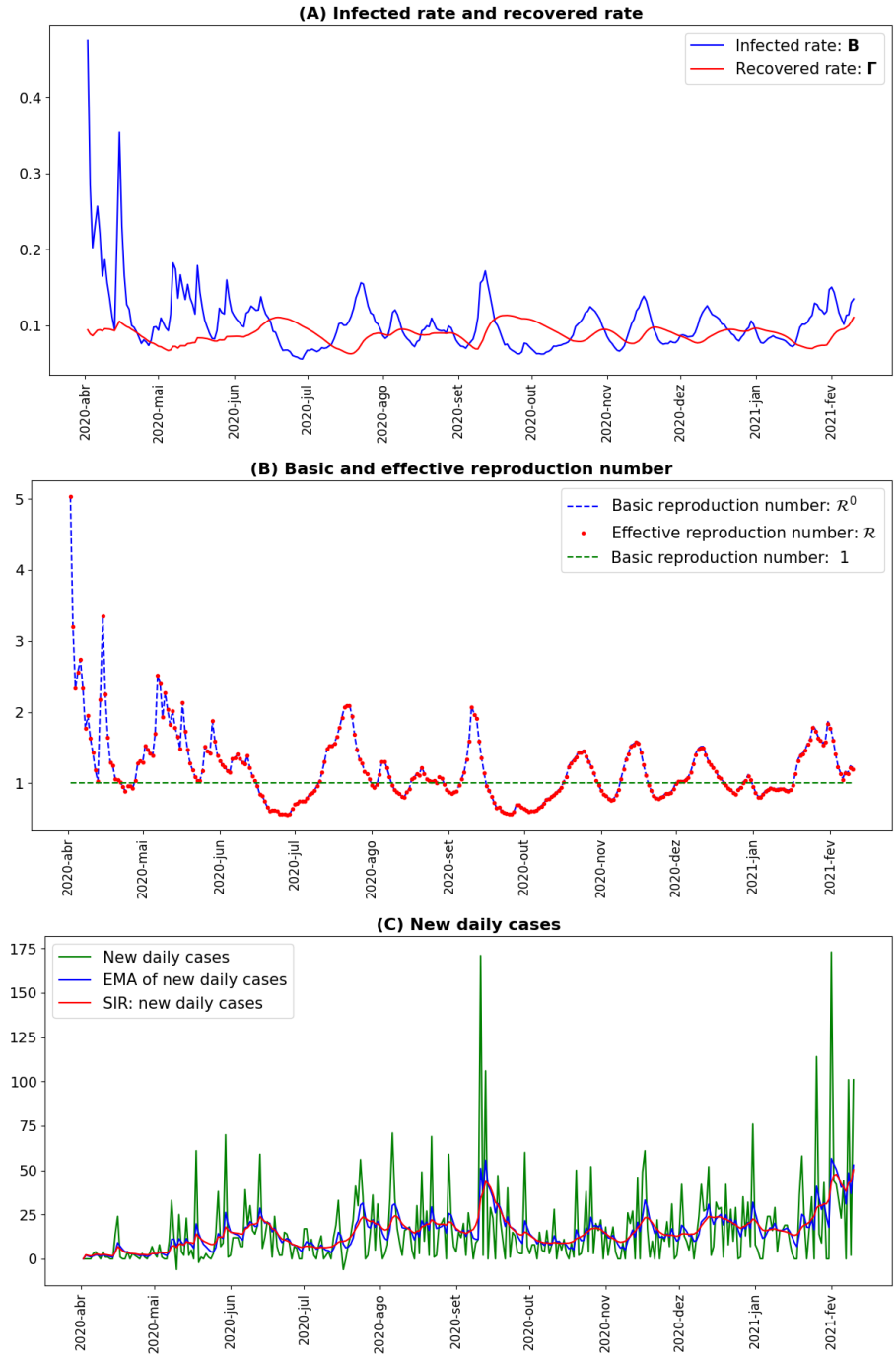

Figure 5: Plots for Petrópolis. See Figure 3 for the subplot description.

Remark 1. *In this paper, we estimate the parameters β_i and γ_i for $i = 1, 2, \ldots, N$ based on known data. Regarding predictions, one could, for instance, use constants β and γ for predictions. In [10], the authors predict pessimistic/optimistic outcomes of up to 70 days based on maximum/minimum values of β of a prior period. In [29], the author employs the Gomperz model combined with an iterative method to estimate future points.*

6 CONCLUSION

Computational modeling yields a powerful helping hand in understanding the dynamics of complex phenomena, but it is often the case that model parameters are not all available. That is the case with epidemiological models, in particular when human activity is involved. Here, we employ a SIR model combined with real data to understand the dynamics of COVID-19 infections. To find out important time dependent parameters modeling the probability of contacts and probability of recovery, we use a minimal error method. This type of scheme yields an iterative way to approximate parameters. There is a caveat however: one of the steps of the algorithm is extremely hard to compute, specially for nonlinear problems as ours. We circumvent such hurdle by carefully constructing auxiliary problems that makes the algorithm feasible.

We show that the scheme is reliable by testing with data from two different Brazilian cities: Rio de Janeiro and Petrópolis. The first one with a population of almost seven million people, and Petrópolis with roughly three hundred thousand people. After approximating the parameters, we use them in the model and reproduce the dynamics of the disease with surprising accuracy. That shows that the estimation of parameters was correct. We point out that the results for both cities were qualitative analogous, indicating that the method does not depend on the population size.

Acknowledgments

The authors acknowledge the financial support of PCI-CNPq (first author) Grant number 301525/2023-4, and FAPERJ (second author) Grants SEI-260003/012979/2021 and SEI-260003/009792/2021.

Funding: The authors acknowledge the financial support of PCI-CNPq (first author) Grant number 301525/2023-4, and FAPERJ (second author) Grants SEI-260003/012979/2021 and SEI-260003/009792/2021.

Competing Interests: The authors declare that they have no conflict of interest.

Data availability: The dataset used in the paper was obtained from the Brazilian Ministry of Health and is publicly available at https://covid.saude.gov.br.

Author Contributions: Both authors participated in the concept, development, analysis and writing of the manuscript.

REFERENCES

[1] E. Acosta-González, J. Andrada-Félix & F. Fernández-Rodríguez. On the evolution of the COVID-19 epidemiological parameters using only the series of deceased. A study of the Spanish out-

break using Genetic Algorithms. *Mathematics and Computers in Simulation*, **197** (2022), 91–104. doi:https://doi.org/10.1016/j.matcom.2022.02.007. URL https://www.sciencedirect.com/science/article/pii/S037847542200060X.

[2] V. Albani, J. Loria, E. Massad & J. Zubelli. COVID-19 underreporting and its impact on vaccination strategies. *BMC Infectious Diseases*, **21**(1) (2021), 1111. doi:10.1186/s12879-021-06780-7. URL https://doi.org/10.1186/s12879-021-06780-7.

[3] V.V. Albani, J. Loria, E. Massad & J.P. Zubelli. The impact of COVID-19 vaccination delay: A data-driven modeling analysis for Chicago and New York City. *Vaccine*, **39**(41) (2021), 6088–6094. doi:https://doi.org/10.1016/j.vaccine.2021.08.098. URL https://www.sciencedirect.com/science/article/pii/S0264410X21011580.

[4] V.V.L. Albani, R.M. Velho & J.P. Zubelli. Estimating, monitoring, and forecasting COVID-19 epidemics: a spatiotemporal approach applied to NYC data. *Scientific Reports*, **11**(1) (2021), 9089. doi:10.1038/s41598-021-88281-w. URL https://doi.org/10.1038/s41598-021-88281-w.

[5] F. Amaral, W. Casaca, C.M. Oishi & J.A. Cuminato. Simulating Immunization Campaigns and Vaccine Protection Against COVID-19 Pandemic in Brazil. *IEEE Access*, **9** (2021), 126011–126022. doi:10.1109/ACCESS.2021.3112036.

[6] F. Amaral, W. Casaca, C.M. Oishi & J.A. Cuminato. Towards Providing Effective Data-Driven Responses to Predict the COVID-19 in São Paulo and Brazil. *Sensors*, **21**(2) (2021), 540. URL https://doi.org/10.3390/s21020540.

[7] C. Anastassopoulou, L. Russo, A. Tsakris & S. C. Data-based analysis, modelling and forecasting of the COVID-19 outbreak. *PLoS ONE*, **15**(3) (2020). doi:https://doi.org/10.1371/journal.pone.0230405.

[8] K. Atkinson & W. Han. "Theoretical numerical analysis", volume 39. Springer (2005).

[9] L. Brotherhood, P. Kircher, C. Santos & M. Tertilt. An Economic Model of the COVID-19 Epidemic: The Importance of Testing and Age-Specific Policies. report 13265, IZA Institute of Labor Economics (2020). URL https://www.iza.org/publications/dp/13265.

[10] E.L. Campos, R.P. Cysne, A.L. Madureira & G.L. Mendes. Multi-generational SIR modeling: Determination of parameters, epidemiological forecasting and age-dependent vaccination policies. *Infectious Disease Modelling*, **6** (2021), 751–765.

[11] W. Chen. A mathematical model of Ebola virus based on SIR model. In "2015 International Conference on Industrial Informatics-Computing Technology, Intelligent Technology, Industrial Information Integration". IEEE (2015), p. 213–216.

[12] J. Chu. A statistical analysis of the novel coronavirus (COVID-19) in Italy and Spain. *PloS one*, **16**(3) (2021), e0249037.

[13] Y. Hao, T. Xu, H. Hu, P. Wang & Y. Bai. Prediction and analysis of corona virus disease 2019. *PloS one*, **15**(10) (2020), e0239960.

[14] H.W. Hethcote. The Mathematics of Infectious Diseases. *SIAM Review*, **42**(4) (2000), 599–653. URL http://www.jstor.org/stable/2653135.

[15] H.G. Hong & Y. Li. Estimation of time-varying reproduction numbers underlying epidemiological processes: A new statistical tool for the COVID-19 pandemic. *PloS one*, **15**(7) (2020), e0236464.

[16] Y.H. Hsieh, S. Ma, J.X.V. Hernandez, V.J. Lee & W.Y. Lim. Early outbreak of 2009 influenza A (H1N1) in Mexico prior to identification of pH1N1 virus. *PLoS One*, **6**(8) (2011).

[17] J. Jahn. "Introduction to the theory of nonlinear optimization". Springer Nature (2020).

[18] B. Kaltenbacher, A. Neubauer & O. Scherzer. "Iterative regularization methods for nonlinear ill-posed problems", volume 6. Walter de Gruyter (2008).

[19] K.M. Kamina, S. Mwalili & A. Wanjoya. The modeling of a stochastic SIR model for HIV/AIDS epidemic using Gillespie's algorithm. *Int. J. Data Sci. Anal*, **5**(6) (2019), 117.

[20] W.O. Kermack & A.G. McKendrick. A contribution to the mathematical theory of epidemics. *Proceedings of the royal society of london. Series A, Containing papers of a mathematical and physical character*, **115**(772) (1927), 700–721.

[21] N. Khan, A. Arshad, M. Azam, A.H. Al-marshadi & M. Aslam. Modeling and forecasting the total number of cases and deaths due to pandemic. *Journal of Medical Virology*, **94**(4) (2022), 1592–1605.

[22] I.E. Kibona & C. Yang. SIR model of spread of Zika virus infections: ZIKV linked to microcephaly simulations. *Health*, **9**(8) (2017), 1190–1210.

[23] B. Li & Z. Eskandari. Dynamical analysis of a discrete-time SIR epidemic model. *Journal of the Franklin Institute*, **360**(12) (2023), 7989–8007.

[24] Z. Liao, P. Lan, Z. Liao, Y. Zhang & S. Liu. TW-SIR: time-window based SIR for COVID-19 forecasts. *Scientific reports*, **10**(1) (2020), 1–15.

[25] A. Neubauer. A new gradient method for ill-posed problems. *Numerical Functional Analysis and Optimization*, **39**(6) (2018), 737–762.

[26] W.C. Roda, M.B. Varughese, D. Han & M.Y. Li. Why is it difficult to accurately predict the COVID-19 epidemic? . *Infectious Disease Modelling*, **5** (2020), 271–281. doi:https://doi.org/10.1016/j.idm.2020.03.001. URL `http://www.sciencedirect.com/science/article/pii/S2468042720300075`.

[27] S. Sannigrahi, F. Pilla, B. Basu, A.S. Basu & A. Molter. Examining the association between socio-demographic composition and COVID-19 fatalities in the European region using spatial regression approach. *Sustainable cities and society*, **62** (2020), 102418.

[28] T.E. Simos, C. Tsitouras, V.N. Kovalnogov, R.V. Fedorov & D.A. Generalov. Real-time estimation of R0 for COVID-19 spread. *Mathematics*, **9**(6) (2021), 664.

[29] J.A.M. Valle. Predicting the number of total COVID-19 cases and deaths in Brazil by the Gompertz model. *Nonlinear Dynamics*, **102**(4) (2020), 2951–2957.

[30] C. You, Y. Deng, W. Hu, J. Sun, Q. Lin, F. Zhou, C.H. Pang, Y. Zhang, Z. Chen & X.H. Zhou. Estimation of the time-varying reproduction number of COVID-19 outbreak in China. *International Journal of Hygiene and Environmental Health*, **228** (2020), 113555.

How to cite

Valle, J.A.M. & Madureira, A.L. Parameter Identification Problem in the discrete-time SIR Model. *Trends in Computational and Applied Mathematics*, **25**(2024), e01805. doi: 10.5540/tcam.2024.025.e01805.

APPENDIX A EXPONENTIAL MOVING AVERAGE (EMA)

The real data indicating the number of daily infected patients is too "rough", and hampers the convergence of the algorithm. That can be avoided by replacing the data $\hat{\boldsymbol{I}}^{cumul}$ with a exponential moving average

$$\hat{\boldsymbol{I}}^{\text{EMA}} = \left(\hat{I}_1^{\text{EMA}}, \hat{I}_2^{\text{EMA}}, \ldots, \hat{I}_N^{\text{EMA}}\right)$$

as described below.

Moving average techniques smooth data over a specified period of time. There is a wide variety of moving averages, and the *Simple Moving Average* (*SMA*), and *Exponential Moving Average* (*EMA*) are of interest.

An EMA gives "more weight" to recent numbers in an attempt to make it more responsive to new information. To calculate an EMA, you first choose a window of d days. In our case, we choose $d = 10$. Then, compute the SMA using the first d days, i.e., simply take the data average of the first d days. Next, it is enough to compute the EMA using appropriate weights. Then, the EMA of the rough data containing the cumulative number of confirmed cases

$$\hat{\boldsymbol{I}}^{rough} = \left(\hat{I}_1^{rough}, \hat{I}_2^{rough}, \ldots, \hat{I}_{N+d}^{rough}\right),$$

follows the formula

$$\hat{I}_j^{cumul} = \begin{cases} \frac{\hat{I}_1^{rough} + \hat{I}_2^{rough} + \ldots + \hat{I}_d^{rough}}{d}, & \text{if } j = 1, \\ \hat{I}_{j+d-1}^{rough}\left(\frac{2}{1+d}\right) + \hat{I}_{j-1}^{cumul}\left(1 - \frac{2}{1+d}\right), & \text{if } j = 2, 3, \ldots, N, \end{cases}$$

and $\hat{I}_j^{cumul}$ represents EMA of $\hat{\boldsymbol{I}}^{rough}$ at day j. Note that the smoothed data "starts" at day $d+1$. Again, we consider $d = 10$.

APPENDIX B MINIMAL ERROR METHOD

In this appendix we outline mathematical details of the Minimal Error Method. Let $F : \mathcal{D}(F) \subset \mathbb{R}^p \to \mathbb{R}^q$ be a nonlinear operator, where $\mathcal{D}(F)$ is domain of F, and $F(\boldsymbol{x}) = (f_1(\boldsymbol{x}), f_2(\boldsymbol{x}), \cdots, f_q(\boldsymbol{x})) = \boldsymbol{y}$. The problem is to estimate $\boldsymbol{x}$, given $\boldsymbol{y}$.

The transpose of a vector $\boldsymbol{x}$ is denoted by $\boldsymbol{x}^T$. The linear continuous operator $F'(\boldsymbol{x}) : \mathbb{R}^p \to \mathbb{R}^q$ is called the Fréchet derivative of F at $\boldsymbol{x}$, and in finite dimensional problems this operator is the Jacobian matrix evaluated at $\boldsymbol{x}^T = (x_1, x_2, \cdots, x_p)$ [8, 17].

The transpose (or adjoint operator) $F'(\boldsymbol{x})^T$ (or $F'(\boldsymbol{x})^*$) of $F'(\boldsymbol{x})$ is an operator $F'(\boldsymbol{x})^T : \mathbb{R}^q \to \mathbb{R}^p$ satisfying

$$\left\langle F'(\boldsymbol{x})^T \boldsymbol{z}, \boldsymbol{w} \right\rangle_{\mathbb{R}^p} = \left\langle \boldsymbol{z}, F'(\boldsymbol{x})\boldsymbol{w} \right\rangle_{\mathbb{R}^q}, \quad \text{for all } \boldsymbol{z} \in \mathbb{R}^q,\ \boldsymbol{w} \in \mathbb{R}^p,$$

where $\langle \boldsymbol{a}, \boldsymbol{b} \rangle_{\mathbb{R}^p} = \boldsymbol{a}^T \boldsymbol{b}$ denotes the inner product of the vectors $\boldsymbol{a}$ and $\boldsymbol{b}$ in $\mathbb{R}^p$.

To obtain an approximation for $\boldsymbol{x}$, given $\boldsymbol{y}$ and guess initial $\boldsymbol{x}^1$, we used the minimal error method

$$\boldsymbol{x}^{k+1} = \boldsymbol{x}^k + \omega^k F'(\boldsymbol{x}^k)^T (\boldsymbol{y} - F(\boldsymbol{x}^k)), \tag{B.1}$$

where the weight

$$\omega_k = \frac{1}{M} \frac{\|\boldsymbol{y} - F(\boldsymbol{x}^k)\|_{\mathbb{R}^p}^2}{\|F'(\boldsymbol{x}^k)^T (\boldsymbol{y} - F(\boldsymbol{x}^k))\|_{\mathbb{R}^q}^2}.$$

Above, $\|\cdot\|_{\mathbb{R}^p}$ is the Euclidean norm and $1/M < 2$; see [25]. In our numerical tests, $M = p$ delivered the best results.

It is possible to show that, under certain conditions, $\boldsymbol{x}^k$ converges to a solution of $F(\boldsymbol{x}) = \boldsymbol{y}$; see [18, Theorem 3.21] or [25, Theorem 2.6].

From iteration (B.1), to get $\boldsymbol{x}^{k+1}$ we need to calculate the transpose of Jacobian matrix $F'(\boldsymbol{x}^k)^T$, that makes the algorithm impractical. In this work, we show that it is possible to calculate $\boldsymbol{x}^{k+1}$ without computing the transpose of the Jacobian matrix.